

Published in final edited form as:

Biochemistry. 2010 March 9; 49(9): 1975–1984. doi:10.1021/bi901867s.

Effect of Calcium-sensitizing Mutations on Calcium Binding and Exchange with Troponin C in Increasingly Complex Biochemical Systems[†]

Svetlana B. Tikunova^{‡,§}, Bin Liu^{‡,||}, Nicholas Swindle[§], Sean C. Little^{||}, Aldrin V. Gomes[⊥], Darl R. Swartz[¶], and Jonathan P. Davis^{||,*}

[§]From the Department of Pharmacological and Pharmaceutical Sciences, University of Houston, Houston, TX 77204

^{||}From the Department of Physiology and Cell Biology, The Ohio State University, Columbus, OH 43210

[⊥]From the Department of Neurobiology, Physiology and Behavior, University of California, Davis, CA 95616

[¶]From the Department of Animal Sciences, Purdue University, West Lafayette, IN 47907

Abstract

The calcium dependent interactions between troponin C (TnC) and other thin and thick filament proteins play a key role in regulation of cardiac muscle contraction. Five hydrophobic residues Phe²⁰, Val⁴⁴, Met⁴⁵, Leu⁴⁸ and Met⁸¹ in the regulatory domain of TnC were individually substituted with polar Gln, to examine the effect of these mutations that sensitized isolated TnC to calcium on: 1) calcium binding and exchange with TnC in increasingly complex biochemical systems and 2) calcium sensitivity of actomyosin ATPase. The hydrophobic residue mutations drastically affected calcium binding and exchange with TnC in increasingly complex biochemical systems, indicating that side chain intra- and inter-molecular interactions of these residues play a crucial role in determining how TnC responds to calcium. However, the mutations that sensitized isolated TnC to calcium did not necessarily increase the calcium sensitivity of the troponin (Tn) complex or reconstituted thin filaments with or without myosin S1. Furthermore, the calcium sensitivity of reconstituted thin filaments (in the absence of myosin S1) was a better predictor of the calcium dependence of actomyosin ATPase activity than that of TnC or the Tn complex. Thus, both the intrinsic properties of TnC and its interactions with the other contractile proteins play a crucial role in modulating calcium binding to TnC in increasingly complex biochemical systems

The processes of cardiac muscle contraction and relaxation can be regulated by multiple physiological and patho-physiological stimuli. It is clear that protein alterations associated with heart disease, isoform switching and post translational modifications can affect both the Ca²⁺ sensitivity of muscle force generation and relaxation kinetics (for review, see (1–4)). Since cardiac troponin C (TnC)¹ is the Ca²⁺ sensor responsible for initiating the contraction / relaxation cycle (for review, see (5,6)), a potentially important mechanism to alter cardiac

[†]This research was funded by NIH grants 5R00HL087462 (to S.B.T) and 5R01HL073828 (to D.R.S.); by Predoctoral Fellowship Award from the American Heart Association (to B. L.) and by National Scientist Development Award from the American Heart Association (to J.P.D).

*Address correspondence to: Jonathan P. Davis, Department of Physiology and Cell Biology, The Ohio State University, 304 Hamilton Hall, 1645 Neil Avenue, Columbus, OH 43210, Tel. 614-247-2559; Fax. 614-292-4888; davis.812@osu.edu.

[‡]These two authors contributed equally to the manuscript

muscle performance is through directly modifying the properties of TnC. As it has been difficult to find specific pharmacological modulators of TnC, we have taken a genetic approach to modify Ca^{2+} binding and exchange with TnC.

In cardiac muscle, TnC functions as a subunit of the troponin (Tn) complex, which also consists of troponin I (TnI) and troponin T (TnT) (for review, see (5–9)). TnC is a dumbbell shaped protein, comprised of the N- and C-terminal globular domains that are connected by a flexible α -helical linker. It is generally accepted that the N-domain regulates muscle contraction/relaxation through the binding and release of Ca^{2+} , while the structural C-domain anchors TnC into the Tn complex. The Tn complex interacts with actin and tropomyosin (Tm) to form the thin filament. At low intracellular $[\text{Ca}^{2+}]$, the C-domain of TnI is thought to bind to actin and prevent the strong, force producing interactions between actin and myosin. An increase in intracellular $[\text{Ca}^{2+}]$ strengthens interactions between the N-domain of TnC and the regulatory C-domain of TnI, causing release of TnI from actin, which results in the movement of Tm on the surface of actin. The movement of Tm then allows myosin to strongly interact with actin to generate force and muscle shortening. Conversely, a decrease in intracellular $[\text{Ca}^{2+}]$ leads to the dissociation of Ca^{2+} and TnI from the N-domain of TnC, which initiates muscle relaxation (for review, see (8,10,11)).

An ultimate goal of our research is to delineate the role of TnC in cardiac muscle physiology. This can be achieved by designing of TnC mutants with desired properties, and examining the effects of these mutations on physiological behavior of muscle. Recently, we designed a series of cardiac TnC^{F27W} mutants that sensitized the regulatory N-domain to Ca^{2+} (up to ~15-fold), by individually substituting hydrophobic residues F20, V44, M45, L48 and M81 with polar Q (12). We hypothesized that the Ca^{2+} sensitization effect was due to the facilitation of the structural transition occurring in the regulatory domain of TnC upon Ca^{2+} binding. Surprisingly, the increase in Ca^{2+} affinity of isolated TnC^{F27W} was mainly due to faster Ca^{2+} association rates (up to ~9-fold) rather than to slower Ca^{2+} dissociation rates (only up to ~3-fold).

As mentioned above, we engineered five individual mutations into the N-domain of TnC that increased the Ca^{2+} binding affinity of isolated TnC^{F27W} (12). However, when these TnC^{F27W} mutants were reconstituted into skinned cardiac trabeculae, $\text{F20QTnC}^{\text{F27W}}$ actually desensitized cardiac muscle to Ca^{2+} (13,14). These results indicate that in muscle additional factors can influence the apparent Ca^{2+} binding properties of TnC. Consistent with this idea, our recent study demonstrated that both thin and thick filament proteins modulate Ca^{2+} binding affinity and kinetics of TnC (15). Therefore, determination of how thin and thick filament proteins affect Ca^{2+} binding and exchange with TnC mutants is crucial when designing TnC constructs with desired properties.

In the present study, the Ca^{2+} affinities and dissociation rates for Ca^{2+} sensitizing TnC mutants were measured in increasingly complex biochemical systems: from the Tn complex to the reconstituted thin filaments with or without myosin S1. The results indicated that hydrophobic side chain intra- and inter-molecular interactions of these residues played an important role in dictating the Ca^{2+} binding properties of TnC in increasingly complex biochemical systems. Furthermore, the Ca^{2+} sensitivity of the reconstituted thin filaments was better at predicting

¹Abbreviations: Tn, troponin; TnC, troponin C; TnI, troponin I; TnT, troponin T; IAANS, 2-(4-(iodoacetamido)anilino)naphthalene-6-sulfonic acid; TnC^{F27W} , human cardiac TnC with F27W mutation; TnC^{F29W} , chicken skeletal TnC with F29W mutation; TnC^{T53C} , Cys-less human cardiac TnC with T53C mutation; TnC^{T53C} , TnC^{T53C} labeled with IAANS; TnI_{128–180}, peptide corresponding to residues from 128 to 180 of human cardiac TnI; EGTA, ethylene glycol-bis(2-aminoethyl)-N,N,N',N'-tetraacetic acid; Quin-2, 2-[[2-bis(carboxymethyl)amino-5-methylphenoxy]methyl]-6-methoxy-8-bis(carboxymethyl)aminoquinoline; DTT, dithiothreitol; MOPS, 3-(N-morpholino)propanesulfonic acid; Tween-20, polysorbate 20; K_d , dissociation constant; SA, surface area

the Ca^{2+} dependence of actomyosin ATPase, compared to that of either isolated TnC or the Tn complex. Thus, both the intrinsic properties of TnC and its interactions with the other contractile proteins play an important role in modulating Ca^{2+} binding and exchange with TnC in increasingly complex biochemical systems.

Experimental Procedures

Materials

Phenyl-Sepharose CL-4B, Tween-20, Sodium Molybdate Dihydrate and EGTA were purchased from Sigma Chemical Co. (St. Louis, MO). Quin-2 was purchased from Calbiochem (La Jolla, CA). IAANS and phalloidin were purchased from Invitrogen (Carlsbad, CA). Affi-Gel 15 affinity media was purchased from Bio-Rad (Hercules, CA). Malachite Green Oxalate and Poly(vinyl Alcohol) were bought from Fisher Scientific (Pittsburgh, PA). The human cardiac TnI peptide (residues 128–180) herein designated as TnI_{128–180} was synthesized and purified by Celtek Peptide Department, Celtek Bioscience LLC (Nashville, TN).

Protein Mutagenesis and Purification

The pET3a plasmid encoding human cardiac TnC was a generous gift from Dr. Lawrence B. Smillie (University of Alberta, Canada). The TnC mutant with C35S, T53C and C84S mutations (herein designated TnC^{T53C}), and its mutants were generated from pET3a TnC plasmid as previously described (15). The mutations were confirmed by DNA sequence analysis. Expression and purification of TnC^{T53C} and its mutants were carried out as previously described (15).

The plasmid encoding human cardiac TnI was transformed into *E. coli* Rosetta™ (DE3)pLysS cells (Novagen, San Diego, CA). Expression of TnI was induced by adding 0.4 mM IPTG when the bacterial cell density reached an OD₆₀₀ of 0.8–1.0. The purification of TnI was carried out utilizing standard laboratory techniques, which included DEAE sepharose chromatography (to absorb DNA, RNA and other contaminants), CM sepharose chromatography, and affinity chromatography on an Affi-Gel 15 column (to which TnC was covalently attached) (16,17).

Human cardiac TnT (isoform 3) was expressed and purified as previously described (18). Rabbit fast skeletal actin and myosin S1; and bovine cTm were isolated, purified and quantified as previously described (15).

Labeling of TnC^{T53C} and its Mutants

TnC^{T53C} and its mutants were labeled with the environmentally sensitive thiol-reactive fluorescent probe IAANS as previously described (15).

Reconstitution of the Tn Complexes

The Tn complexes were prepared and reconstituted as previously described (15).

Reconstitution of the Thin Filaments

After exhaustive dialysis against reconstitution buffer (10 mM MOPS, 150 mM KCl, 3 mM MgCl₂, 1 mM DTT at pH 7.0), actin was mixed with an equal molar ratio of phalloidin to stabilize the actin filaments. Thin filaments were prepared and reconstituted as previously described (15). Briefly, actin-phalloidin (4 μM) and cTm (0.57 μM) were mixed in the reconstitution buffer and kept on ice for ~ 20 minutes. The Tn complexes (0.5 μM) were subsequently added and the thin filaments were kept on ice for ~ 15 minutes before use. To examine the effect of myosin binding on the Ca^{2+} binding properties of the thin filament, myosin S1 (1.14 μM) was subsequently added and kept on ice for ~ 3 minutes before use. Thus,

the stoichiometry for the reconstituted thin filaments was 7:1:0.88:2 (actin/cTm/Tn/myosin S1).

Determination of Ca²⁺ Binding Sensitivities

All steady-state fluorescence measurements were performed using a Perkin-Elmer LS55 spectrofluorimeter at 15°C. IAANS fluorescence was excited at 330 nm and monitored at 450 nm as microliter amounts of CaCl₂ were added to 2 ml of each labeled Tn complex (0.15 μM) in titration buffer (200 mM MOPS (to prevent pH changes upon addition of Ca²⁺), 150 mM KCl, 2 mM EGTA, 1 mM DTT, 3 mM MgCl₂, 0.02% Tween-20, pH 7.0) at 15°C with constant stirring. Reconstituted thin filaments were prepared as described above, and diluted in half with an appropriate solution to achieve identical titration buffer composition (excluding Tween-20). The [Ca²⁺]_{free} was calculated using the computer program EGCA02 developed by Robertson and Potter (19). The Ca²⁺ sensitivities of conformational changes were reported as a dissociation constant K_d, representing a mean of three to four separate titrations ± SE. The data were fit with a logistic sigmoid function (mathematically equivalent to the Hill equation), as previously described (20).

Determination of Ca²⁺ Dissociation Kinetics

All kinetic measurements were performed utilizing an Applied Photophysics Ltd. (Leatherhead, UK) model SX.18 MV stopped-flow instrument with a dead time of ~1.4 ms at 15°C. The rates of conformational changes induced by EGTA removal of Ca²⁺ from labeled Tn complexes or thin filaments were measured following IAANS fluorescence. IAANS was excited at 330 nm. The IAANS emission was monitored through either a 420–470 nm band-pass interference filter or 510 nm broad band-pass interference filter from Oriel (Stratford, CT); or 415–490 nm band-pass interference filter from Newport (Irvine, CA). The composition of stopped-flow buffer was 10 mM MOPS, 150 mM KCl, 1 mM DTT, 3 mM MgCl₂, 0.02 % Tween-20, pH 7.0. The buffer used in the stopped-flow experiments for the reconstituted thin filaments excluded Tween-20. To obtain the data traces, 200 μM CaCl₂ was added to the Tn complexes (0.5 μM) or to the reconstituted thin filaments ± myosin S1 and rapidly mixed with buffer containing 10 mM EGTA. The data were corrected for scattering artifacts as described previously (15). The data were fit using a program (by P. J. King, Applied Photophysics Ltd) that utilizes the nonlinear Levenberg-Marquardt algorithm. Each k_{off} represents an average of at least three separate experiments, each averaging at least five traces fit with a single exponential equation.

Determination of TnI_{128–180} Peptide Affinities

IAANS fluorescence was monitored with excitation at 330 nm and emission at 450 nm. Microliter amounts of TnI_{128–180} were added to 2 ml of each labeled TnC mutant (0.15 μM) in titration buffer at 15°C with constant stirring. Each apparent peptide affinity represents a mean of three to six titrations ± SE fit to the root of a quadratic equation for binary complex formation as previously described (21).

Actomyosin S1 ATPase Assay

Reconstituted thin filaments (5 μM actin, 1.0 μM Tm, 1.5 μM Tn and 0.2 μM myosin S1) were formed at 22°C in a buffer containing 50 mM MOPS, 5 mM MgCl₂, at pH 7.0. EGTA (to a final concentration of 0.5 mM) and various amounts of CaCl₂ were added to the 100 μL reaction mixture aliquots to achieve the desired pCas. The reactions were initiated by adding ATP (to a final concentration of 1 mM). 15 μL aliquots of the reaction mixture were terminated at 4 min. time intervals by addition of ice cold PCA (to a final concentration of 4 %). ATPase activity was determined by analyzing the amount of phosphate released during a time course

of up to 20 minutes. The malachite green assay was utilized to quantify the phosphate released during the reaction as previously described (22).

Calculation of Distances between Residues

Distances between residues were calculated from the four Ca^{2+} saturated Tn crystal structures available from the Protein Data Bank (1J1D and 1J1E (23)) using the computer software Rasmol (24). Residues in TnC were considered to be interacting with residues in TnI if atoms within the residues of these two proteins came within 4\AA of one another.

Calculation of Solvent-accessible Surface Areas

GETAAREA (25) was used to approximate the percent of total surface area (SA) of hydrophobic residues in TnC that are in contact with TnI residues C-terminal to residue 145 (TnI₁₄₆₋₂₁₀). The average SA for each hydrophobic residue was tabulated from the four Ca^{2+} saturated Tn crystal structures available from the protein data bank (1J1D and 1J1E (23)). The percent of total SA for each of the five residues in contact with TnI₁₄₆₋₂₁₀ was calculated as the SA of the residue (side chain and backbone contributions in \AA^2) in contact with TnI₁₄₆₋₂₁₀ divided by the total SA (side chain and backbone contribution in \AA^2) of all twenty-nine residues in contact with TnI₁₄₆₋₂₁₀, with the resulting quotient multiplied by 100.

Statistical Analysis

Statistical significance was determined by an unpaired two-sample t-test using the statistical analysis software Minitab (State College, PA). The two means were considered to be significantly different when the P value was < 0.05 . All data is shown as a mean value \pm S.E..

Results

Effect of TnC Mutations on the Ca^{2+} Sensitivities of the Tn Complexes

Previously, we designed five individual mutations, F20Q, V44Q, M45Q, L48Q and M81Q (Fig. 1) that sensitized the N-domain of isolated TnC to Ca^{2+} (12). The goal of the present work was to examine the effect of these mutations on Ca^{2+} binding and functional properties of TnC in increasingly complex biochemical systems. First, we wanted to examine how these mutations affected the Ca^{2+} sensitivity of the Tn complex. The Ca^{2+} induced decreases in IAANS fluorescence, which occurs when Ca^{2+} binds to the regulatory domain of TnC^{T53C}_{IAANS} and its mutants reconstituted into the Tn complex (Tn^{T53C}_{IAANS}) are shown in Fig. 2A. Tn^{T53C}_{IAANS} exhibited a half-maximal Ca^{2+} dependent decrease in IAANS fluorescence at 634 ± 46 nM (Fig. 2A and Table 1). For the rest of the mutant Tn complexes, Ca^{2+} induced half-maximal decreases in IAANS fluorescence ranged from 260 ± 6 nM for L48QTn^{T53C}_{IAANS} to 28096 ± 3614 nM for F20QTn^{T53C}_{IAANS}. The Hill coefficients for all of the Tn complexes were < 1.0 , indicating an absence of Ca^{2+} binding cooperativity (26). Thus, substitution of hydrophobic residues in positions 20, 44, 45, 48 or 81 of TnC with polar Q produced mutant Tn complexes with up to ~ 2.4 -fold higher and ~ 44 -fold lower Ca^{2+} binding sensitivities, compared to that of Tn^{T53C}_{IAANS}. The results indicate that increasing the Ca^{2+} affinity of isolated TnC does not necessarily sensitize the Tn complex to Ca^{2+} .

Effect of TnC Mutations on the Rates of Ca^{2+} Dissociation from the Tn Complexes

Fluorescence stopped-flow measurements were conducted to determine the effect of five mutations on the kinetics of Ca^{2+} dissociation from Tn^{T53C}_{IAANS}. Fig. 2B shows that the rate of Ca^{2+} dissociation from Tn^{T53C}_{IAANS} measured by following an increase in IAANS fluorescence was

at $41.5 \pm 0.4/s$. The fluorescent Ca^{2+} chelator quin-2 was utilized to measure the rate of Ca^{2+} dissociation from the unlabeled Tn^{T53C} complex at $\sim 38.2 \pm 0.6/s$ (data not shown), which was similar to the value we have previously reported for the regulatory N-domain of the wild-type Tn complex under identical experimental conditions (15). These results indicate that the increase in IAANS fluorescence occurs simultaneously with the actual Ca^{2+} dissociation rate from the regulatory N-domain of the Tn_{IAANS}^{T53C} complex. For the rest of the mutant Tn_{IAANS}^{T53C} complexes, the rates of Ca^{2+} dissociation measured by following increases in IAANS fluorescence ranged from $7.0 \pm 0.1/s$ for L48QTn_{IAANS}^{T53C} to $108 \pm 2/s$ for F20QTn_{IAANS}^{T53C} (Fig. 2B and Table 1). Thus, substitution of hydrophobic residues in positions 20, 44, 45, 48 or 81 of TnC with polar Q produced mutant Tn complexes with up to ~ 5.9 -fold slower and ~ 2.6 -fold faster rates of Ca^{2+} dissociation, compared to that of Tn_{IAANS}^{T53C} .

Effect of TnC Mutations on the TnI_{128–180} Binding Properties of the Ca^{2+} Saturated TnC

A change in the IAANS fluorescence of Ca^{2+} saturated TnC_{IAANS}^{T53C} was utilized to determine the effect of the mutations on the affinity of TnC for the TnI peptide corresponding to residues 128–180 of human cardiac TnI (TnI_{128–180}). Cardiac TnI_{128–180} peptide is homologous to the skeletal TnI_{96–148} peptide, previously shown to be a good model system to study the Ca^{2+} -dependent interactions between skeletal TnI and skeletal TnC (21,27). Fig. 3 demonstrates that the affinity of Ca^{2+} saturated TnC_{IAANS}^{T53C} for TnI_{128–180} was at $\sim 200 \pm 16$ nM. For the rest of the mutants, the affinities for TnI_{128–180} ranged from 262 ± 3 nM for V44QTn_{IAANS}^{T53C} to 437 ± 30 nM for M81QTn_{IAANS}^{T53C} (Fig. 3 and Table 1). Thus, substitution of hydrophobic residues in positions 20, 44, 45, 48 or 81 of TnC with polar Q reduced the affinity of TnC_{IAANS}^{T53C} for TnI_{128–180} by ~ 1.3 – 2.2 -fold.

Effect of TnC Mutations on the Ca^{2+} Binding Sensitivities of the Thin Filaments

The Ca^{2+} induced changes in IAANS fluorescence, which occurs when Ca^{2+} binds to the regulatory domain of Tn_{IAANS}^{T53C} and its mutants reconstituted into the thin filaments are shown in Fig. 4A. Thin filament bound Tn_{IAANS}^{T53C} exhibited a half-maximal Ca^{2+} dependent increase in IAANS fluorescence at 5027 ± 97 nM. For the rest of the mutant Tn complexes reconstituted into the thin filaments, Ca^{2+} induced half-maximal changes in IAANS fluorescence ranged from 168 ± 7 nM for L48QTn_{IAANS}^{T53C} to 6803 ± 604 nM for F20QTn_{IAANS}^{T53C} (Fig. 4A and Table 2). Thus, hydrophobic residue mutations led up to ~ 30 -fold higher and ~ 1.4 -fold lower Ca^{2+} binding sensitivities, compared to that of Tn_{IAANS}^{T53C} reconstituted thin filaments. For three of the mutations (F20Q, M45Q and L48Q) as well as TnC_{IAANS}^{T53C} , the incorporation of the Tn complexes into the thin filaments led to a positive cooperative Ca^{2+} binding process. The Hill coefficients for the two remaining mutant Tn complexes (with V44Q and M81Q mutations) reconstituted into the thin filaments were ≤ 1.0 , indicating an absence of Ca^{2+} binding cooperativity.

Effect of TnC Mutations on the Rates of Ca^{2+} Dissociation from the Thin Filaments

Fluorescence stopped-flow measurements were conducted to determine the effect of TnC mutations on the kinetics of Ca^{2+} dissociation from the thin filament reconstituted with Tn_{IAANS}^{T53C} . Fig. 4B shows that the rate of Ca^{2+} dissociation from the thin filament reconstituted with Tn_{IAANS}^{T53C} was at $102 \pm 1/s$. For the rest of the TnC mutants, rates of Ca^{2+} dissociation from the reconstituted thin filaments ranged from $22.2 \pm 0.3/s$ for V44QTn_{IAANS}^{T53C} to $221 \pm 12/s$ for F20QTn_{IAANS}^{T53C} (Fig. 4B and Table 2). Thus, hydrophobic residue mutations led up to ~ 4.6 -fold

slower and ~2.2-fold faster rates of Ca^{2+} dissociation from the reconstituted thin filaments, compared to that of $\text{Tn}_{\text{IAANS}}^{\text{T53C}}$ reconstituted thin filaments.

Effect of TnC Mutations on the Ca^{2+} Binding Sensitivities of Thin Filaments In the Presence of Myosin S1

The Ca^{2+} induced change in IAANS fluorescence, which occurs when Ca^{2+} binds to the regulatory domain of $\text{Tn}_{\text{IAANS}}^{\text{T53C}}$ reconstituted thin filaments, in the presence of two myosin S1 per stoichiometric unit, is shown in Fig. 5A. In the presence of myosin S1, $\text{Tn}_{\text{IAANS}}^{\text{T53C}}$ exhibited a half-maximal Ca^{2+} dependent change in IAANS fluorescence at 1007 ± 72 nM. For the rest of the mutants, Ca^{2+} induced half-maximal changes in IAANS fluorescence ranged from 241 ± 11 nM for L48QTn_{IAANS}^{T53C} to 8598 ± 250 nM for F20QTn_{IAANS}^{T53C} (Fig. 5A and Table 2). The Hill coefficients for all of the Tn complexes reconstituted into the thin filaments in the presence of myosin S1 were ≤ 1.0 , indicating an absence of Ca^{2+} binding cooperativity. Thus, in the presence of myosin S1, Ca^{2+} binding sensitivities of the thin filaments reconstituted with mutant Tn complexes were up to ~4.2-fold higher and ~8.5-fold lower, compared to that of $\text{Tn}_{\text{IAANS}}^{\text{T53C}}$ bound thin filaments.

Effect of TnC Mutations on the Rates of Ca^{2+} Dissociation from the Thin Filaments in the Presence of Myosin S1

Fluorescence stopped-flow measurements were conducted to determine the effect of the mutations on the kinetics of Ca^{2+} dissociation from the thin filaments in the presence of myosin S1. In the presence of two myosin S1 per stoichiometric unit, the rate of Ca^{2+} dissociation from the thin filaments reconstituted with $\text{Tn}_{\text{IAANS}}^{\text{T53C}}$ was at $\sim 12.6 \pm 0.1/\text{s}$ (Fig. 5B). For the rest of the mutations, the rates of Ca^{2+} dissociation ranged from $\sim 2.1 \pm 0.1/\text{s}$ for L48QTn_{IAANS}^{T53C} to $42 \pm 1/\text{s}$ for F20QTn_{IAANS}^{T53C} (Fig. 5B and Table 2). Thus, in the presence of myosin S1, the Ca^{2+} dissociation rate from the thin filaments for the five different mutations ranged from ~6.0-fold slower to ~3.3-fold faster.

Effect of TnC Mutations on the Ca^{2+} Dependence of Actomyosin ATPase

To examine the functional effect of TnC mutations, the Ca^{2+} dependence of actomyosin ATPase activity was measured in the thin filaments reconstituted with $\text{Tn}_{\text{IAANS}}^{\text{T53C}}$ or mutants. The specific ATPase activity at pCa 9.0 of $\text{Tn}_{\text{IAANS}}^{\text{T53C}}$ was 0.015 ± 0.001 (mol P_i/s)/mol S1 (Fig. 6A and Table 3). For the rest of the mutations, the specific ATPase activity at pCa 9.0 was ~1.3–1.9-fold higher than that of $\text{Tn}_{\text{IAANS}}^{\text{T53C}}$ (Fig. 6A and Table 3). The specific ATPase activity at pCa 4.0 of $\text{Tn}_{\text{IAANS}}^{\text{T53C}}$ was 0.059 ± 0.001 (mol P_i/s)/mol S1 (Fig. 6A and Table 3). For the rest of the mutations, the specific ATPase activity at pCa 4.0 was up to ~1.6-fold lower than that of $\text{Tn}_{\text{IAANS}}^{\text{T53C}}$ (Fig. 6A and Table 3). For $\text{Tn}_{\text{IAANS}}^{\text{T53C}}$, half-maximal activation occurred at 969 ± 53 nM (Fig. 6B and Table 3). The F20Q mutation affected the ability of TnC to both inhibit ATPase in the absence of Ca^{2+} , and to activate ATPase in the presence of Ca^{2+} , preventing us from determining the effect of this mutation on the Ca^{2+} sensitivity of actomyosin ATPase. For V44Q, M45Q, L48Q and M81Q mutations, half-maximal activation ranged from 158 ± 11 nM for L48QTn_{IAANS}^{T53C} to 1173 ± 254 nM for M81QTn_{IAANS}^{T53C} (not significantly different from that of $\text{Tn}_{\text{IAANS}}^{\text{T53C}}$) (Fig. 6B and Table 3). Thus, TnC mutations caused up to ~6.1-fold increases in the Ca^{2+} sensitivity of actomyosin ATPase.

Discussion

The main objective of this study was to examine how mutations that sensitized isolated TnC to Ca^{2+} affect the Ca^{2+} binding and functional properties of TnC in increasingly complex biochemical systems. Previously, we utilized the F27W substitution to follow Ca^{2+} binding and exchange with the second EF-hand of isolated TnC (12). We individually substituted F20, V44, M45, L48 and M81 with polar Q, to design five TnC^{F27W} mutants with increased sensitivity to Ca^{2+} (12). Residues V44 and M81 are located on the A and D helices (within the NAD unit), while residues V44, M45 and L48 are located on the B helix (within the BC unit) (Fig. 7). In both the absence and presence of Ca^{2+} , the side chains of these five residues are involved in extensive hydrophobic interactions between the NAD and BC units. These inter-unit hydrophobic interactions are lost in the Tn complex, as the BC unit moves away from the NAD unit in order to bind to the C-terminal domain of TnI (Fig. 7). Thus, we reasoned that substitution of either one of these hydrophobic residues with polar Q should lead to the higher Ca^{2+} sensitivity of the N-domain of TnC, by facilitating the movement of the BC unit away from the NAD unit. Indeed, individual substitutions of these residues with Q increased Ca^{2+} affinity of the N-domain of TnC ~ 2.1–15.3-fold. The increases in Ca^{2+} affinity were largely due to faster Ca^{2+} association rates (~2.6–8.7-fold faster) rather than to slower Ca^{2+} dissociation rates (only ~1.2–2.9-fold slower)(12). The Ca^{2+} sensitizing effect of these five mutations was not caused by the fluorescent W27 reporter, since these mutations also led to ~2.4–23.0-fold increases in the Ca^{2+} affinity of the N-domain of TnC^{C35S} labeled with IAANS on C84 (28). Thus, we believe that outcomes observed in our earlier study were attributed to the mutations of hydrophobic residues to Q and not to the F27W substitution.

Due to the presence of W residues in other regulatory muscle proteins, we were unable to utilize the F27W substitution to follow Ca^{2+} binding and exchange with TnC reconstituted into the Tn complex or the thin filaments. Thus, the fluorescence of $\text{TnC}_{\text{IAANS}}^{\text{T53C}}$ was utilized to follow Ca^{2+} binding and exchange with the regulatory N-domain of TnC and its mutants in biochemical systems of increasing complexity. Unlike TnC labeled on either of the endogenous C35 or C84 residues, $\text{TnC}_{\text{IAANS}}^{\text{T53C}}$ remains spectroscopically sensitive to Ca^{2+} binding after TnC is reconstituted into the Tn complex, and the thin filaments both in the absence and presence of myosin S1 (15). Since extrinsic labeling of C53 with IAANS could have modified the Ca^{2+} binding properties of TnC and affected its physiological function, the effects of labeling were carefully considered (15). Measurements of Ca^{2+} dissociation from the $\text{Tn}_{\text{IAANS}}^{\text{T53C}}$ complex as monitored by the IAANS fluorescence and by quin-2 fluorescence from unlabeled Tn^{T53C} and wild-type Tn complexes yielded similar rates (15). The Ca^{2+} affinity of the $\text{Tn}_{\text{IAANS}}^{\text{T53C}}$ complex was similar to the K_d of ~300–700 nM previously reported for unlabeled wild-type reconstituted Tn and native bovine cardiac Tn complexes (29). In addition, the Ca^{2+} affinity of the reconstituted thin filaments was similar to the K_d of ~ 1.7–5 μM previously reported for native cardiac bovine thin filaments (30). Furthermore, the ability of $\text{TnC}_{\text{IAANS}}^{\text{T53C}}$ to develop Ca^{2+} dependent force in skinned trabeculae was similar to that of wild-type and endogenous TnC (15). These results indicated that labeling of C53 with IAANS minimally affected the Ca^{2+} binding properties of TnC.

The five TnC mutants studied in the present work exhibited ~108-, 40- and 36-fold variation in the Ca^{2+} sensitivities of the Tn complexes, reconstituted thin filaments without and with myosin S1, respectively. Furthermore, the five TnC mutants also exhibited ~15-, 10- and 20-fold variation in the rates of Ca^{2+} dissociation from the Tn complexes, reconstituted thin filaments without and with myosin S1, respectively. These results indicate that hydrophobic side chain intra- and inter-molecular interactions of these residues play an important role in dictating the Ca^{2+} binding properties of TnC in increasingly complex biochemical systems.

This interpretation of the results is based on the assumption that the IAANS fluorescence directly reflects Ca^{2+} binding to the TnC mutants. Alternatively, the probe might reflect conformational changes occurring in the N-domain of TnC mutants subsequent to Ca^{2+} binding. Additional experiments, including structural studies, are currently under way to more fully characterize the TnC mutants.

Analysis of the four available crystal structures of the core domain of cardiac Tn (23) indicated that all five hydrophobic residues could play an important role in binding to the regulatory domain of TnI. Of the twenty-nine TnC residues that form a contact surface between the regulatory domains of TnC and TnI, these five hydrophobic residues account for a disproportionately large $31.6 \pm 0.2\%$ of the contact area. The side chains of F20, V44, L48, M45 and M81 in TnC come in close contact with the side chains of several hydrophobic residues (I148, A150, A152, M153, M154, A156 and L157) in TnI. However, the five individual mutations only modestly decreased TnI_{128–180} binding affinity ~1.3–2.2-fold, with the F20Q and M81Q mutations having the largest effect on peptide affinity. Consistent with this finding, the homologous mutants of skeletal TnC^{F29W} displayed ~1.7–3.0-fold lower affinity for skeletal TnI_{96–148}, with the homologues of F20Q and M81Q having the largest effect on peptide affinity (21). One possible explanation of a modest effect of these TnC mutations on the peptide affinity is that other residues are able to compensate for the loss of one hydrophobic interaction between the mutated side-chain of TnC and the residues in TnI. Alternatively, electrostatic interactions could play an integral role in determining the affinity of TnC for TnI.

All five hydrophobic mutations sensitized isolated TnC to Ca^{2+} (12), but only L48Q substitution sensitized the Tn complex to Ca^{2+} . In fact, F20Q, V44Q, M45Q and M81Q mutations led to ~1.3–44.3-fold lower Ca^{2+} sensitivity of the Tn complex. Thus, mutations that sensitize isolated TnC to Ca^{2+} do not necessarily increase the Ca^{2+} sensitivity of the Tn complex. The binding of TnI stabilizes the “open” state of the N-domain of TnC (31,32), drastically increasing the affinity of TnC for Ca^{2+} (33). Possibly, the hydrophobic residue mutations mimic the effects of TnI binding by shifting the equilibrium of the N-domain of TnC from the “closed” toward the “open” state, facilitating Ca^{2+} binding. Thus, binding of TnI does not have the same Ca^{2+} sensitizing effect on these mutants as it does on wild-type TnC. The BC unit hydrophobic residue mutations V44Q, M45Q and L48Q led up to ~5.9-fold slower, while NAD unit mutations F20Q and M81Q led up to ~2.6-fold faster rate of Ca^{2+} dissociation from the Tn complex (~15-fold variation in the rate of Ca^{2+} dissociation). Thus, mutations of hydrophobic residues had a larger effect on the rates of Ca^{2+} dissociation from the Tn complex than on that of isolated TnC (15). The faster rates of Ca^{2+} dissociation caused by F20Q and M81Q mutations suggest that these mutations destabilized the Ca^{2+} bound state of the Tn complex. Analysis of the four crystal structures of the core domain of the Tn (23) indicates that the side chain of F20 interacts with the side chain of M81 in the Ca^{2+} saturated N-domain of TnC reconstituted into the Tn complex (Fig. 7). Thus, substitution of either one of these residues with polar Q could affect interactions between the A and D-helices, destabilizing the Ca^{2+} bound state of TnC reconstituted into the Tn complex.

As mentioned above, while all five hydrophobic mutations sensitized isolated TnC to Ca^{2+} (12), only the L48Q substitution increased the Ca^{2+} sensitivity of the Tn complex. On the other hand, V44Q, M45Q, L48Q and M81Q substitutions led to ~1.1–30.0-fold higher Ca^{2+} sensitivity of the reconstituted thin filaments. These results are consistent with a competition between TnC and actin for the C-terminal domain of TnI (for review see (34)). Possibly, actin decreases the probability of TnC-TnI interactions, allowing V44Q, M45Q, L48Q and M81Q mutations to sensitize the thin filaments to Ca^{2+} , since these mutations sensitized isolated TnC to Ca^{2+} . Alternatively, the hydrophobic residue mutations could have destabilized the interactions between helix H4 of TnI (residues 164–188) and actin, due to reduced hydrophobic interactions between helix H3 of TnI (residues 150–159) and the regulatory N-domain of TnC.

The fact that hydrophobic residue mutations resulted in the increase of the basal activity of actomyosin ATPase provides indirect support for this interpretation.

Interestingly, binding of myosin S1 to the thin filaments reconstituted with F20QTn^{T53C}_{IAANS*}, M45QQTn^{T53C}_{IAANS*} and L48QTn^{T53C}_{IAANS*} actually led to ~1.3–1.8-fold decreases in Ca²⁺ affinity, contrasting with ~5.0-fold increase in Ca²⁺ affinity caused by myosin S1 binding to the thin filaments reconstituted with Tn^{T53C}_{IAANS*}. One possible explanation is that myosin binding to actin causes conformational rearrangements in regulatory proteins, ultimately leading to the increased probability of TnC-TnI interactions. Increased probability of TnC-TnI interactions would lead to the increased Ca²⁺ sensitivity of the thin filament bound TnC^{T53C}_{IAANS*} but not necessarily of TnC mutants which are not as sensitized to Ca²⁺ by TnI binding as TnC^{T53C}_{IAANS*}. Additionally, the mutations could have affected interactions between TnC and TnT, ultimately leading to altered interactions of the thin filaments with myosin S1.

The Ca²⁺ sensitivity of TnC in isolation or reconstituted into the Tn complex is not always a good predictor of physiological outcome (22,35–37). To examine the functional effects of TnC mutations, the Ca²⁺ dependence of actomyosin ATPase was measured after reconstitution of thin filaments with Tn^{T53C}_{IAANS*} or its mutants. Consistent with the effect of V44Q and L48Q mutations on the Ca²⁺ sensitivity of the thin filaments (both in the absence or presence of myosin S1), these two mutations sensitized actomyosin ATPase to Ca²⁺. While the M45Q mutation did not have a significant effect on the Ca²⁺ sensitivity of the thin filaments in the presence of myosin S1, this mutation sensitized both the thin filaments (in the absence of myosin S1) and actomyosin ATPase to Ca²⁺. Additionally, the M81Q substitution had almost no effect on the Ca²⁺ sensitivity of the thin filaments (in the absence of myosin S1), and did not significantly affect the Ca²⁺ sensitivity of actomyosin ATPase.

We were unable to determine the effect of the F20Q mutation on the Ca²⁺ dependence of actomyosin ATPase, as this mutation affected the ability of TnC to inhibit ATPase in the absence of Ca²⁺ and to activate ATPase in the presence of saturating Ca²⁺. Further structural studies might be necessary to decipher why this mutation has detrimental effects on ability of TnC to regulate ATPase. However, even though the F20Q mutation significantly decreased maximal actomyosin ATPase activity, it was previously shown to only moderately decrease the maximal isometric tension development by TnC^{F27W} reconstituted into skinned cardiac trabeculae (13). Similarly, several skeletal TnC^{F29W} mutants significantly reduced maximal ATPase activity without affecting maximal isometric tension development by TnC^{F29W} reconstituted into skinned skeletal muscle (38). In addition to a moderate reduction in maximal force recovery, the F20Q mutation was previously shown to produce ~1.5-fold decrease in the Ca²⁺ sensitivity of force development (13), correlating with ~1.4-fold decrease in the Ca²⁺ sensitivity of the thin filaments in the absence of myosin S1 observed in the present work. Thus, our data indicate that reconstituted thin filaments (in the absence of myosin S1) were better than either isolated TnC or the Tn complex in predicting the functional effect of the mutations. These results are in agreement with those observed for TnI mutants linked to hypertrophic or restricted cardiomyopathies (22), and for TnC mutants linked to hypertrophic or dilated cardiomyopathies (37).

On the other hand, while V44Q, M45Q and L48Q increased the Ca²⁺ sensitivity of the thin filaments in the absence of myosin S1 to a varying extent (~6.0–29.9-fold increases), all three mutations produced similar ~4.9–6.1-fold increases in the Ca²⁺ sensitivity of ATPase. However, the effect of the mutations on Ca²⁺ binding properties of the thin filaments was evaluated only under the conditions of unbound myosin or rigor bound myosin, not in the presence of cycling cross-bridges. Rigor and cycling cross-bridges have been shown to exert

different effects on the Ca^{2+} dependent changes in the Tn structure (39). However, it was not possible to evaluate the effect of hydrophobic residue mutations on the Ca^{2+} binding properties of the thin filaments in the presence of cycling cross-bridges under the physiological salt concentration used in the present work. Likely, cycling cross-bridges attenuate the effect of the mutations on Ca^{2+} sensitivity of the thin filaments, leading to the Ca^{2+} dependence of actomyosin ATPase observed in this work.

In summary, fluorescence of $\text{TnC}^{\text{T53C}}_{\text{IAANS}}$ was utilized to follow Ca^{2+} binding and exchange with the regulatory N-domain of TnC. The F20Q, V44Q, M45Q, L48Q and M81Q mutations were then individually engineered into the N-domain of TnC to determine the effect of these mutations on Ca^{2+} binding properties of TnC in increasingly complex biochemical systems. The five mutations modestly decreased the affinity of TnC for the regulatory region of TnI. However, the five mutations drastically affected Ca^{2+} binding and exchange with TnC in increasingly complex biochemical systems, indicating that hydrophobic side chain intra- and inter-molecular interactions of these residues play a crucial role in dictating how TnC responds to Ca^{2+} . The effect of the mutations on the Ca^{2+} sensitivity of increasingly complex biochemical systems, or actomyosin ATPase, could not always be predicted from their effect on isolated TnC. In fact, while all five mutations increased the Ca^{2+} affinity of isolated TnC, only three mutations increased the Ca^{2+} sensitivity of actomyosin ATPase. However, the Ca^{2+} sensitivity of reconstituted thin filaments (in the absence of myosin S1) was a better indicator than that of the isolated TnC or the Tn complexes of the effect of these mutations on the Ca^{2+} dependence of actomyosin ATPase. In conclusion, examining the effects of the Ca^{2+} sensitizing mutations on Ca^{2+} binding and exchange with TnC in increasingly complex biochemical systems enhances understanding of how TnC responds to Ca^{2+} to regulate muscle function.

Acknowledgments

We wish to thank Dr. Lawrence Smillie (University of Alberta) for the generous gift of the human cardiac TnC and TnI plasmids, and Kristopher Kline (The Ohio State University) for technical assistance. We wish to thank Dr. James D. Potter (University of Miami Miller School of Medicine) for his support and encouragement during the course of this work. We also wish to thank Dr. Jack A. Rall (The Ohio State University) for his support and encouragement during the course of this work.

References

1. Metzger JM, Westfall MV. Covalent and noncovalent modification of thin filament action: the essential role of troponin in cardiac muscle regulation. *Circ Res* 2004;94:146–158. [PubMed: 14764650]
2. Li MX, Wang X, Sykes BD. Structural based insights into the role of troponin in cardiac muscle pathophysiology. *J Muscle Res Cell Motil* 2004;25:559–579. [PubMed: 15711886]
3. Davis JP, Tikunova SB. Ca^{2+} exchange with troponin C and cardiac muscle dynamics. *Cardiovasc Res* 2008;77:619–626. [PubMed: 18079104]
4. Gomes AV, Potter JD. Molecular and cellular aspects of troponin cardiomyopathies. *Ann N Y Acad Sci* 2004;1015:214–224. [PubMed: 15201162]
5. Farah CS, Reinach FC. The troponin complex and regulation of muscle contraction. *Faseb J* 1995;9:755–767. [PubMed: 7601340]
6. Filatov VL, Katrukha AG, Bulargina TV, Gusev NB. Troponin: structure, properties, and mechanism of functioning. *Biochemistry (Mosc)* 1999;64:969–985. [PubMed: 10521712]
7. Gomes AV, Potter JD, Szczesna-Cordary D. The role of troponins in muscle contraction. *IUBMB Life* 2002;54:323–333. [PubMed: 12665242]
8. Tobacman LS. Thin filament-mediated regulation of cardiac contraction. *Annu Rev Physiol* 1996;58:447–481. [PubMed: 8815803]
9. Kobayashi T, Jin L, de Tombe PP. Cardiac thin filament regulation. *Pflugers Arch* 2008;457:37–46. [PubMed: 18421471]

10. Gordon AM, Homsher E, Regnier M. Regulation of contraction in striated muscle. *Physiol Rev* 2000;80:853–924. [PubMed: 10747208]
11. Gordon AM, Regnier M, Homsher E. Skeletal and cardiac muscle contractile activation: tropomyosin "rocks and rolls". *News Physiol Sci* 2001;16:49–55. [PubMed: 11390948]
12. Tikunova SB, Davis JP. Designing calcium-sensitizing mutations in the regulatory domain of cardiac troponin C. *J Biol Chem* 2004;279:35341–35352. [PubMed: 15205455]
13. Norman C, Rall JA, Tikunova SB, Davis JP. Modulation of the rate of cardiac muscle contraction by troponin C constructs with various calcium binding affinities. *Am J Physiol Heart Circ Physiol* 2007;293:H2580–H2587. [PubMed: 17693547]
14. Tikunova SB, Alionte C, Gomes AV, Potter JD, Rall JA, Davis JP. Effect of cardiac troponin C mutations on calcium binding and exchange with the troponin complex and muscle force generation. *Biophys J Abstract Issue* 2006:A117–A118.
15. Davis JP, Norman C, Kobayashi T, Solaro RJ, Swartz DR, Tikunova SB. Effects of thin and thick filament proteins on calcium binding and exchange with cardiac troponin C. *Biophys J* 2007;92:3195–3206. [PubMed: 17293397]
16. Kluwe L, Maeda K, Maeda Y. E. coli expression and characterization of a mutant troponin I with the three cysteine residues substituted. *FEBS Lett* 1993;323:83–88. [PubMed: 8495752]
17. Guo X, Wattanapernpool J, Palmiter KA, Murphy AM, Solaro RJ. Mutagenesis of cardiac troponin I. Role of the unique NH₂-terminal peptide in myofilament activation. *J Biol Chem* 1994;269:15210–15216. [PubMed: 8195157]
18. Gomes AV, Venkatraman G, Davis JP, Tikunova SB, Engel P, Solaro RJ, Potter JD. Cardiac troponin T isoforms affect the Ca²⁺ sensitivity of force development in the presence of slow skeletal troponin I: insights into the role of troponin T isoforms in the fetal heart. *J Biol Chem* 2004;279:49579–49587. [PubMed: 15358779]
19. Robertson S, Potter JD. The regulation of free Ca²⁺ ion concentration by metal chelators. *Methods in Pharmacology* 1984;5:63–75.
20. Tikunova SB, Rall JA, Davis JP. Effect of hydrophobic residue substitutions with glutamine on Ca²⁺ binding and exchange with the N-domain of troponin C. *Biochemistry* 2002;41:6697–6705. [PubMed: 12022873]
21. Davis JP, Rall JA, Alionte C, Tikunova SB. Mutations of hydrophobic residues in the N-terminal domain of troponin C affect calcium binding and exchange with the troponin C-troponin I96–148 complex and muscle force production. *J Biol Chem* 2004;279:17348–17360. [PubMed: 14970231]
22. Kobayashi T, Solaro RJ. Increased Ca²⁺-affinity of cardiac thin filaments reconstituted with cardiomyopathy-related mutant cardiac troponin I. *J Biol Chem*. 2006
23. Takeda S, Yamashita A, Maeda K, Maeda Y. Structure of the core domain of human cardiac troponin in the Ca²⁺-saturated form. *Nature* 2003;424:35–41. [PubMed: 12840750]
24. Sayle RA, Milner-White EJ. RASMOL: biomolecular graphics for all. *Trends Biochem Sci* 1995;20:374. [PubMed: 7482707]
25. Fraczekiewicz R, Braun W. Exact and efficient analytical calculation of the accessible surface area and their gradient for macromolecules. *Journal of Computational Chemistry* 1998;19:319–333.
26. Grabarek Z, Grabarek J, Leavis PC, Gergely J. Cooperative binding to the Ca²⁺-specific sites of troponin C in regulated actin and actomyosin. *J Biol Chem* 1983;258:14098–14102. [PubMed: 6643469]
27. Davis JP, Rall JA, Reiser PJ, Smillie LB, Tikunova SB. Engineering competitive magnesium binding into the first EF-hand of skeletal troponin C. *J Biol Chem* 2002;277:49716–49726. [PubMed: 12397067]
28. Tikunova SB, Davis JP, Rall JA. Engineering cardiac troponin C (cTnC) mutants with dramatically altered Ca²⁺ dissociation rates as molecular tools to study cardiac muscle relaxation. *Biophys J* 2004;86:394. (abstr.).
29. Holroyde MJ, Robertson SP, Johnson JD, Solaro RJ, Potter JD. The calcium and magnesium binding sites on cardiac troponin and their role in the regulation of myofibrillar adenosine triphosphatase. *J Biol Chem* 1980;255:11688–11693. [PubMed: 6449512]
30. Tobacman LS, Sawyer D. Calcium binds cooperatively to the regulatory sites of the cardiac thin filament. *J Biol Chem* 1990;265:931–939. [PubMed: 2136850]

31. Li MX, Spyropoulos L, Sykes BD. Binding of cardiac troponin-I147–163 induces a structural opening in human cardiac troponin-C. *Biochemistry* 1999;38:8289–8298. [PubMed: 10387074]
32. Dong WJ, Xing J, Villain M, Hellinger M, Robinson JM, Chandra M, Solaro RJ, Umeda PK, Cheung HC. Conformation of the regulatory domain of cardiac muscle troponin C in its complex with cardiac troponin I. *J Biol Chem* 1999;274:31382–31390. [PubMed: 10531339]
33. Johnson JD, Collins JH, Robertson SP, Potter JD. A fluorescent probe study of Ca²⁺ binding to the Ca²⁺-specific sites of cardiac troponin and troponin C. *J Biol Chem* 1980;255:9635–9640. [PubMed: 7430090]
34. Kobayashi T, Solaro RJ. Calcium, thin filaments, and the integrative biology of cardiac contractility. *Annu Rev Physiol* 2005;67:39–67. [PubMed: 15709952]
35. Pinto JR, Parvatiyar MS, Jones MA, Liang J, Ackerman MJ, Potter JD. A functional and structural study of troponin C mutations related to hypertrophic cardiomyopathy. *J Biol Chem* 2009;284:19090–19100. [PubMed: 19439414]
36. Reece KL, Moss RL. Intramolecular interactions in the N-domain of cardiac troponin C are important determinants of calcium sensitivity of force development. *Biochemistry* 2008;47:5139–5146. [PubMed: 18410130]
37. Dweck D, Hus N, Potter JD. Challenging current paradigms related to cardiomyopathies Are changes in the Ca²⁺ sensitivity of myofilaments containing cardiac troponin C mutations (G159D and L29Q) good predictors of the phenotypic outcomes? *J Biol Chem* 2008;283:33119–33128. [PubMed: 18820258]
38. Chandra M, da Silva EF, Sorenson MM, Ferro JA, Pearlstone JR, Nash BE, Borgford T, Kay CM, Smillie LB. The effects of N helix deletion and mutant F29W on the Ca²⁺ binding and functional properties of chicken skeletal muscle troponin. *J Biol Chem* 1994;269:14988–14994. [PubMed: 8195134]
39. Sun YB, Lou F, Irving M. Calcium- and myosin-dependent changes in troponin structure during activation of heart muscle. *J Physiol* 2009;587:155–163. [PubMed: 19015190]
40. Spyropoulos L, Li MX, Sia SK, Gagne SM, Chandra M, Solaro RJ, Sykes BD. Calcium-induced structural transition in the regulatory domain of human cardiac troponin C. *Biochemistry* 1997;36:12138–12146. [PubMed: 9315850]

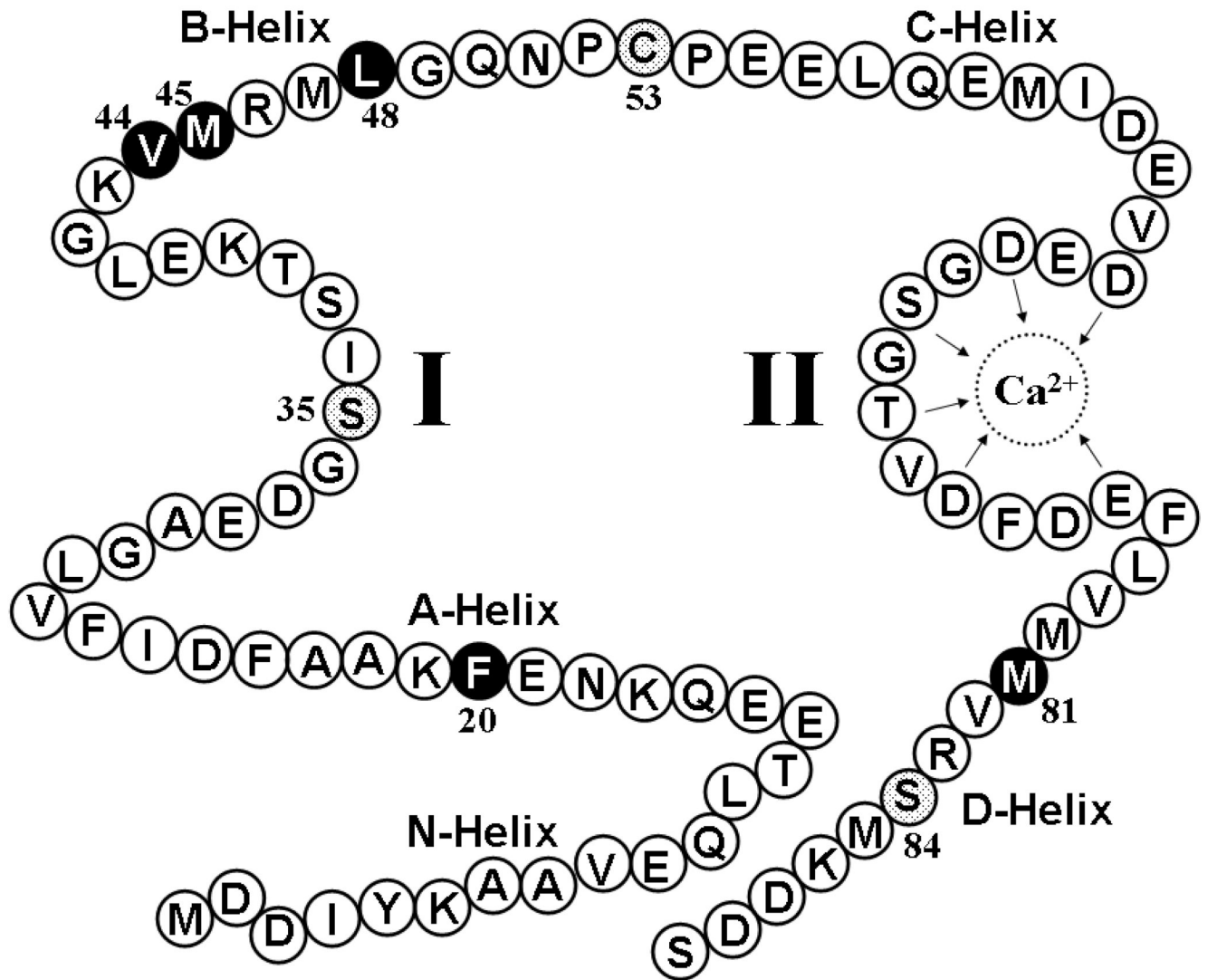


Figure 1. Schematic representation of the regulatory domain of TnC^{T53C}

The figure depicts the amino acids in the regulatory N-domain of TnC^{T53C} (residues 1–89) of TnC that form the defunct site I, the functional Ca²⁺ binding site II, and the various helices (N–D). The black circles represent the hydrophobic residues that were individually substituted with Q, whereas the dot filled circles represent the residues C35, T53 and C84 that were mutated in order to specifically label TnC^{T53C} with IAANS.

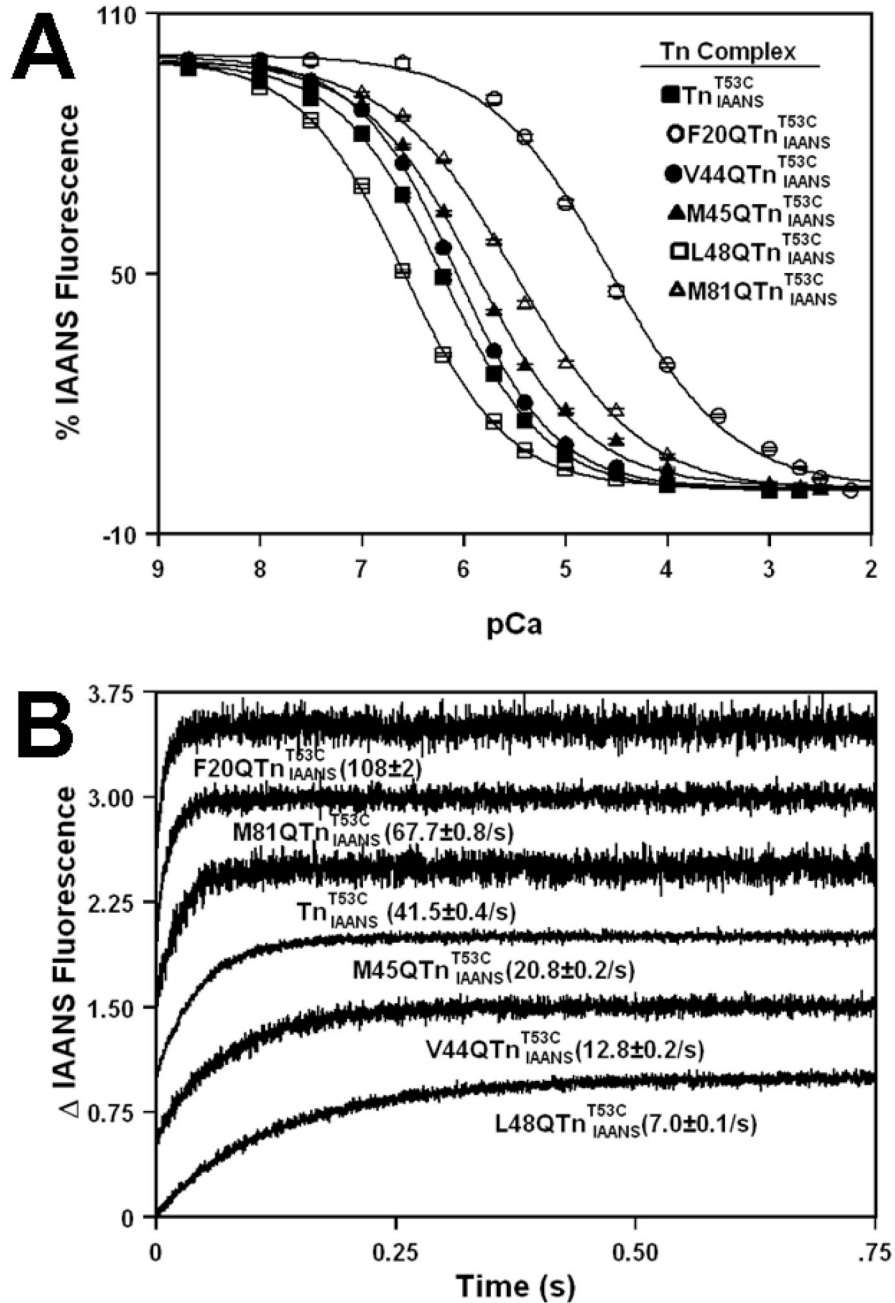


Figure 2. Effect of TnC mutations on the Ca²⁺ binding properties of Tn complexes

Panel A shows the Ca²⁺ dependent decreases in IAANS fluorescence for Tn^{T53C}_{IAANS} (■), F20QTn^{T53C}_{IAANS} (○), V44QTn^{T53C}_{IAANS} (●), M45QTn^{T53C}_{IAANS} (▲), L48QTn^{T53C}_{IAANS} (□) and M81QTn^{T53C}_{IAANS} (△) as a function of pCa. IAANS fluorescence was excited at 330 nm and monitored at 450 nm. The data sets were normalized individually for each mutant. Each data point represents the mean ± S.E. of three titrations fit with a logistic sigmoid function. Panel B shows the time courses of the increase in IAANS fluorescence as Ca²⁺ was removed by EGTA from Tn^{T53C}_{IAANS}, F20QTn^{T53C}_{IAANS}, V44QTn^{T53C}_{IAANS}, M45QTn^{T53C}_{IAANS}, L48QTn^{T53C}_{IAANS} and M81QTn^{T53C}_{IAANS}.

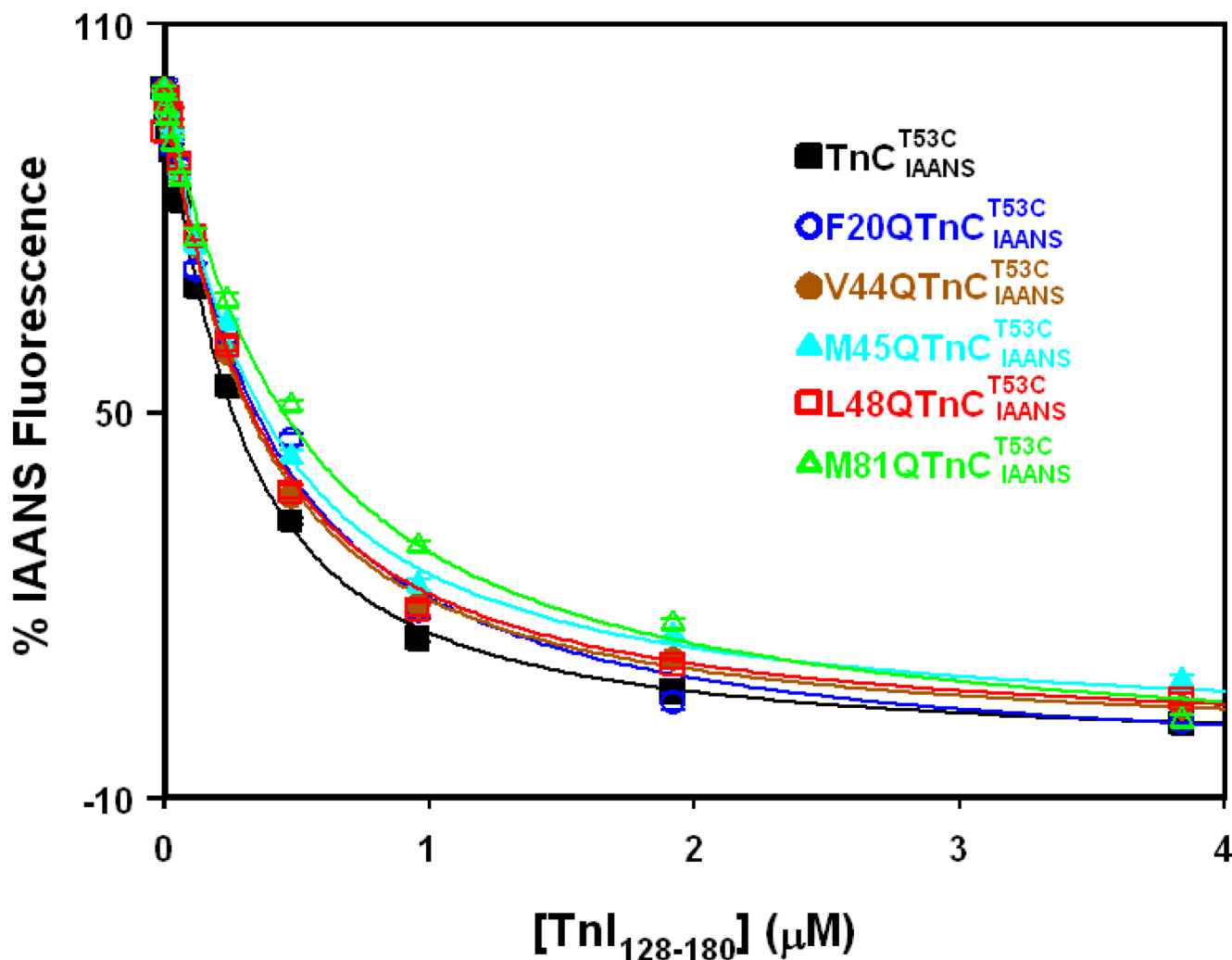


Figure 3. Effect of TnC mutations on TnI₁₂₈₋₁₈₀ binding affinity of TnC

Figure shows the effect of TnC mutations on the TnI₁₂₈₋₁₈₀ binding properties of the Ca²⁺ saturated TnC. The concentration of TnC or its mutants was at 0.15 μM. The TnI₁₂₈₋₁₈₀ dependent changes in IAANS fluorescence are shown as a function of [TnI₁₂₈₋₁₈₀] for Ca²⁺ saturated TnC^{T53C}_{IAANS} (black ■), F20QTnC^{T53C}_{IAANS} (blue ○), V44QTnC^{T53C}_{IAANS} (brown ●), M45QTnC^{T53C}_{IAANS} (cyan ▲), L48QTnC^{T53C}_{IAANS} (red □) and M81QTnC^{T53C}_{IAANS} (green △). 100% IAANS fluorescence corresponds to the Ca²⁺-saturated state, whereas 0% corresponds to the Ca²⁺-InI₁₂₈₋₁₈₀ saturated state for each individual TnC protein. In the case of V44QTnC^{T53C}_{IAANS}, the IAANS fluorescence increased upon addition of TnI₁₂₈₋₁₈₀, so the plot of the data was inverted for comparison purposes. Each data point represents the mean ± S.E. of three to six titrations fit to the root of quadratic equation for binary complex formation.

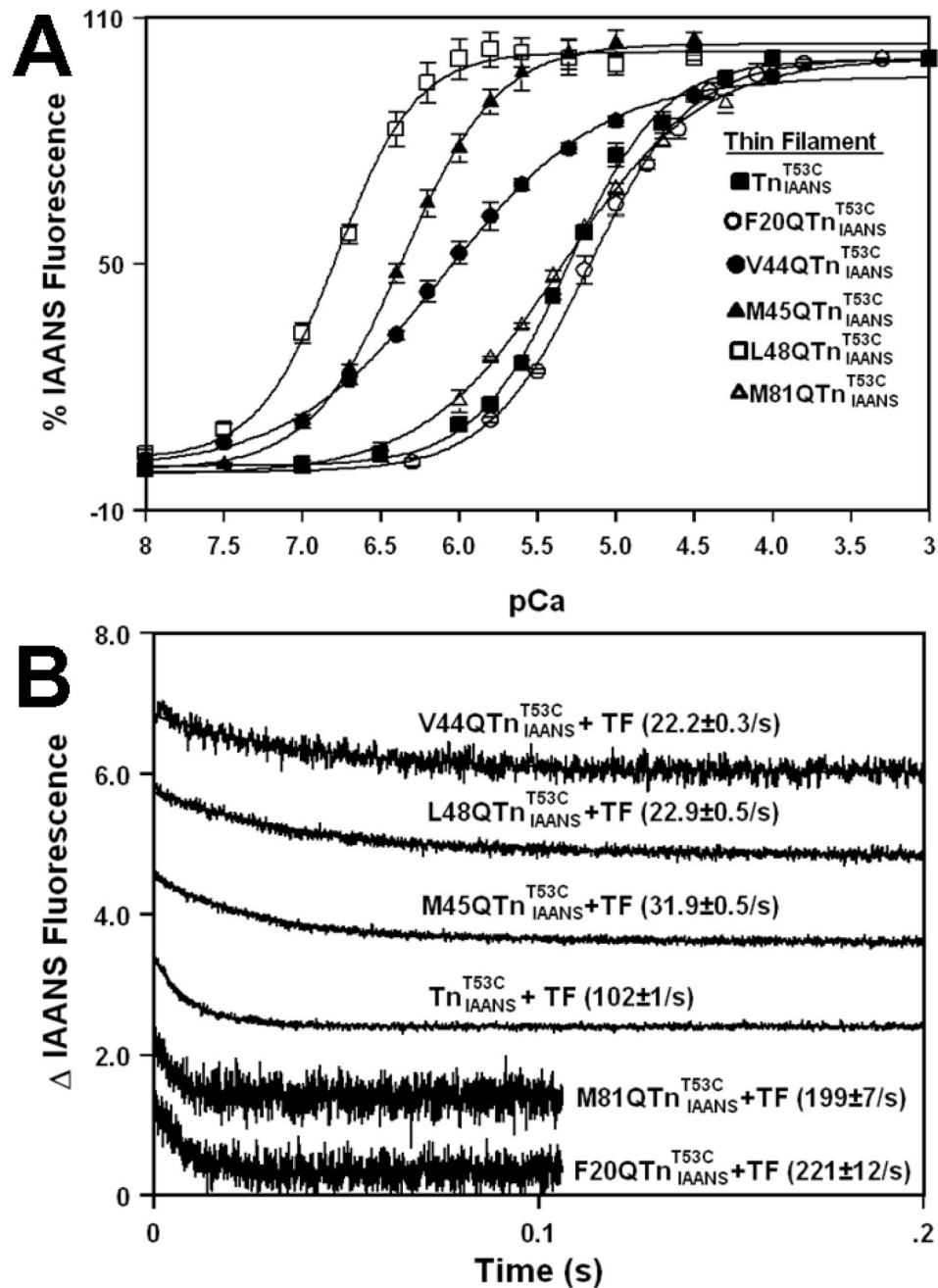


Figure 4. Effect of TnC mutations on the Ca^{2+} binding properties of thin filaments

Panel A shows the Ca^{2+} dependent changes in IAANS fluorescence for Tn_{IAANS}^{T53C} (■), $F20QTn_{IAANS}^{T53C}$ (○), $V44QTn_{IAANS}^{T53C}$ (●), $M45QTn_{IAANS}^{T53C}$ (▲), $L48QTn_{IAANS}^{T53C}$ (□) and $M81QTn_{IAANS}^{T53C}$ (△) reconstituted thin filaments as a function of pCa. The data sets were normalized individually for each mutant. In the case of $V44QTn_{IAANS}^{T53C}$ the IAANS fluorescence decreased upon addition of Ca^{2+} , so the plot of the data was inverted for comparison purposes. Each data point represents the mean \pm S.E. of three to four titrations fit with a logistic sigmoid function. The IAANS fluorescence was excited at 330 nm and monitored at 450 nm. Panel B shows the time courses

of the change in IAANS fluorescence as Ca^{2+} was removed by EGTA from $\text{Tn}_{\text{IAANS}}^{\text{T53C}}$, $\text{F20QTn}_{\text{IAANS}}^{\text{T53C}}$, $\text{V44QTn}_{\text{IAANS}}^{\text{T53C}}$, $\text{M45QTn}_{\text{IAANS}}^{\text{T53C}}$, $\text{L48Tn}_{\text{IAANS}}^{\text{T53C}}$, and $\text{M81QTn}_{\text{IAANS}}^{\text{T53C}}$ reconstituted thin filaments. The data traces have been staggered and normalized for clarity. Each trace is an average of at least five traces fit with a single exponential equation. The IAANS fluorescence was excited at 330 nm and monitored through a 510 nm broad band-pass interference filter. In the case of $\text{V44QTn}_{\text{IAANS}}^{\text{T53C}}$ the IAANS fluorescence was monitored through a 415–490 band-pass interference filter and increased upon removal of Ca^{2+} , so the data traces were inverted for comparison purposes.

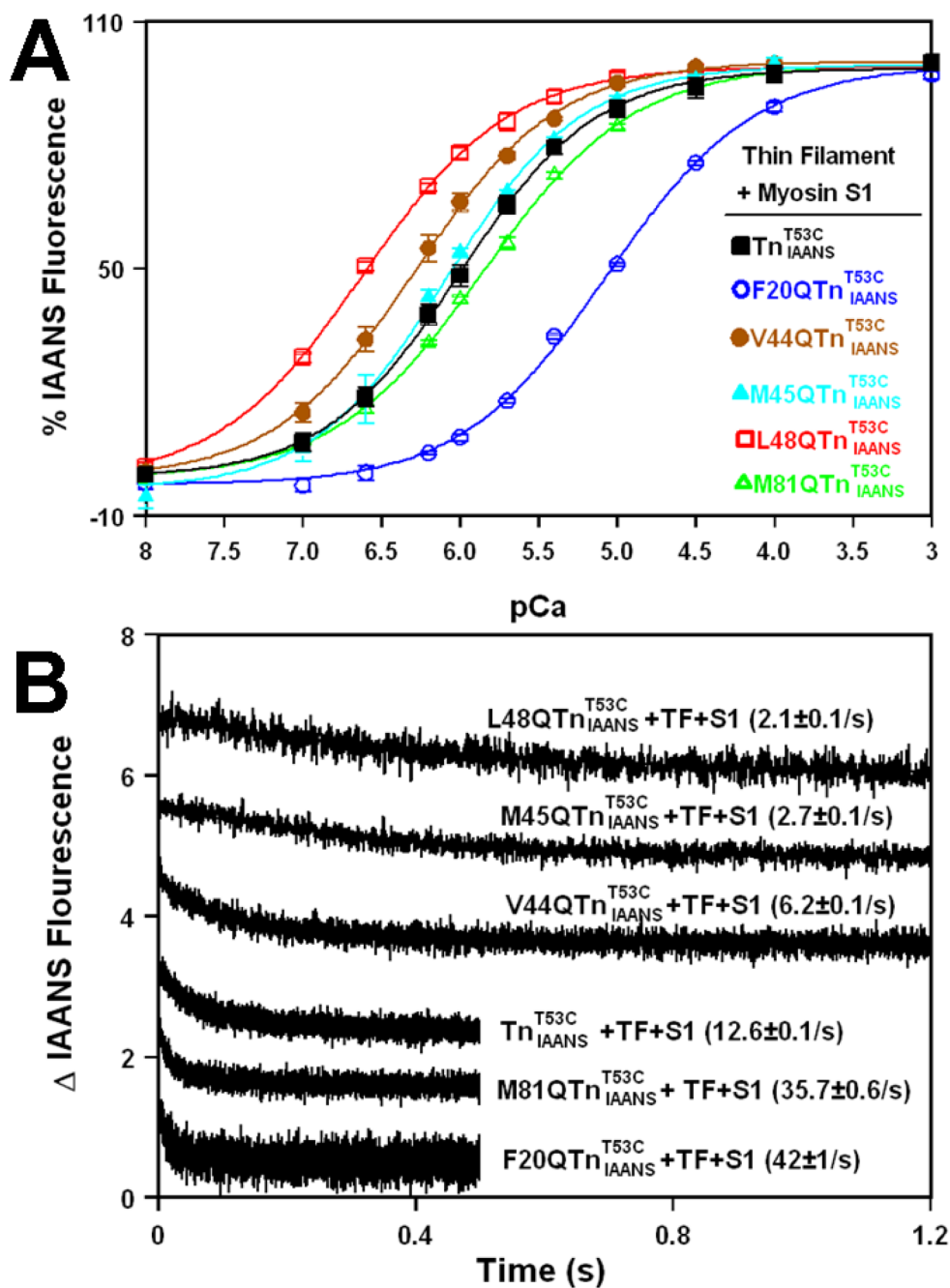


Figure 5. Effect of TnC mutations on the Ca^{2+} binding properties of thin filaments in the presence of myosin S1

Panel A shows the Ca^{2+} dependent changes in IAANS fluorescence for Tn_{IAANS}^{T53C} (black ■), $F20QTn_{IAANS}^{T53C}$ (blue ○), $V44QTn_{IAANS}^{T53C}$ (brown ●), $M45QTn_{IAANS}^{T53C}$ (cyan ▲), $L48QTn_{IAANS}^{T53C}$ (red □) and $M81QTn_{IAANS}^{T53C}$ (green △) reconstituted thin filaments in the presence of myosin S1 as a function of pCa. The data sets were normalized individually for each mutant. Each data point represents the mean \pm S.E. of three to four titrations fit with a logistic sigmoid function. Panel B shows the time courses of the change in IAANS fluorescence as Ca^{2+} was removed by EGTA

from Tn_{IAANS}^{T53C}, F20QTn_{IAANS}^{T53C}, V44QTn_{IAANS}^{T53C}, M45QTn_{IAANS}^{T53C}, L48QTn_{IAANS}^{T53C} and M81QTn_{IAANS}^{T53C} reconstituted thin filaments in the presence of myosin S1. In the case of and the F20QTn_{IAANS}^{T53C} V44QTn_{IAANS}^{T53C} and the M81QTn_{IAANS}^{T53C} the IAANS fluorescence increased upon removal of Ca²⁺, so the data traces were inverted for comparison purposes. The data traces have been staggered and normalized for clarity. Each trace is an average of at least five traces fit with a single exponential equation. The IAANS fluorescence was excited at 330 nm and monitored through a 510 nm broad band-pass interference filter, excluding the F20QTn_{IAANS}^{T53C} V44QTn_{IAANS}^{T53C} and M81QTn_{IAANS}^{T53C} experiments, in which the emission was monitored through a 415–490 nm band-pass interference filter.

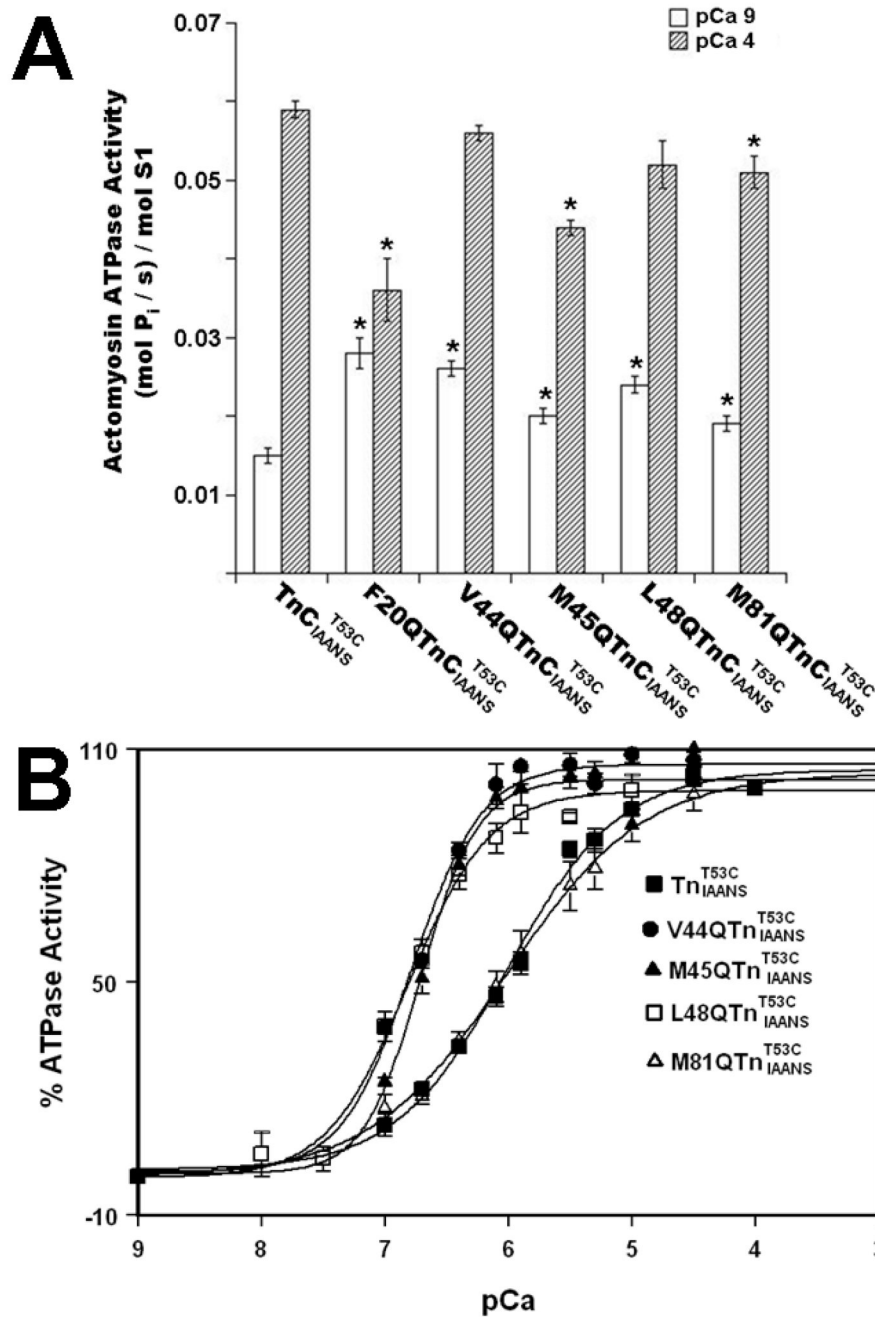


Figure 6. Effect of TnC mutations on the Ca²⁺ dependence of actomyosin ATPase

Panel A shows the specific actomyosin ATPase activities of Tn_{IAANS}^{T53C}, F20QTn_{IAANS}^{T53C}, V44QTn_{IAANS}^{T53C}, M45QTn_{IAANS}^{T53C}, L48QTn_{IAANS}^{T53C}, and M81QTn_{IAANS}^{T53C} at pCa 9.0 (open bars) and pCa 4.0 (bars filled with slanted lines). Each data point represents a mean \pm S.E. of three to six measurements. Values marked with an * are significantly different from their respective control values ($P < 0.05$). Panel B shows the Ca²⁺ dependent activity of actomyosin ATPase for the thin filaments reconstituted with Tn_{IAANS}^{T53C} (■), V44QTn_{IAANS}^{T53C} (●), M45QTn_{IAANS}^{T53C} (▲), L48QTn_{IAANS}^{T53C} (□) and M81QTn_{IAANS}^{T53C} (△) as a function of pCa. Each data point represents a mean \pm S.E. of

three to six measurements. The data sets were individually normalized for each mutant, taking the specific activities at pCa 9.0 as 0% and at pCa 4.0 as 100%, and fit with logistic sigmoid. The experimental conditions were as described under “Experimental Procedures” section.

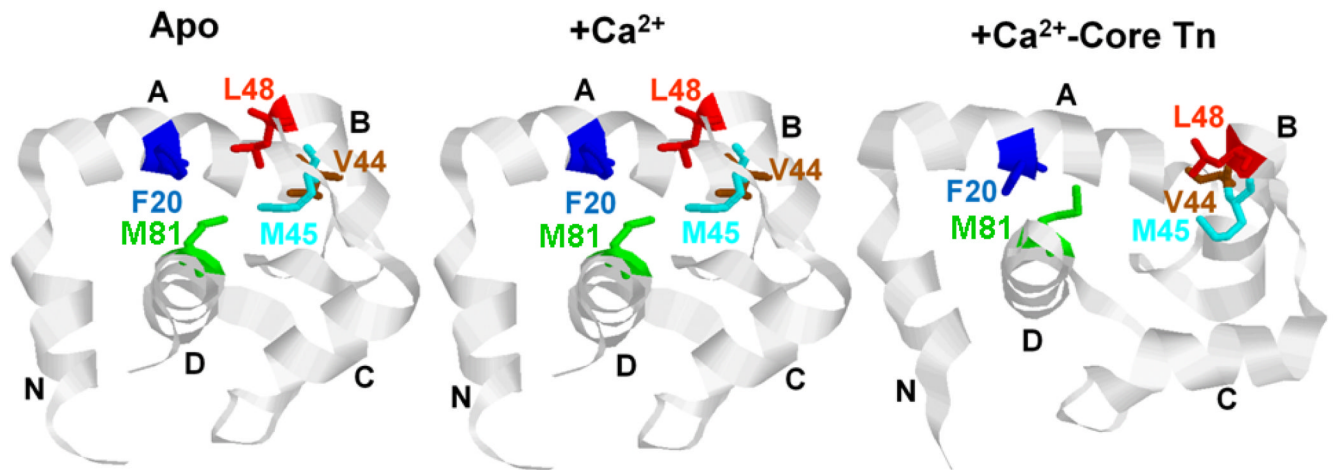


Figure 7. Location of hydrophobic residue mutations in the regulatory N-domain of TnC

A ribbon representation of the N-domain of TnC in the apo state (1SPY(40)) is shown on the left; in the Ca²⁺ bound state (1AP4 (40)) is shown in the middle; and in the Ca²⁺ saturated Tn state (1J1E (23), TnI and TnT have been omitted for clarity) is shown on the right. The helices are labeled (N, A, B, C, and D); while hydrophobic residues that were mutated (F20, V44, M45, L48 and M81) are shown in a ball-and-stick format and labeled. The figure was generated using Rasmol (24).

Table 1

Effects of TnC mutations on the Ca²⁺; binding properties of Tn mutant complexes; and TnI₁₂₈₋₁₈₀ binding affinities.

Protein	Tn complex Ca ²⁺ K _d (nM)	Tn complex Hill coefficient	Tn complex Ca ²⁺ K _{off} (/s)	TnC TnI ₁₂₈₋₁₈₀ K _d , (nM)
TnC ^{T53C} _{IAANS}	634 ± 46	0.86±0.04	41.5±0.4	200±16
F20QTnC ^{T53C} _{IAANS}	28096±3614*	0.73±0.03	108±2*	318±29*
V44QTnC ^{T53C} _{IAANS}	845±9*	0.89±0.01	12.8±0.2*	262±3*
M45QTnC ^{T53C} _{IAANS}	1331±75*	0.78±0.01	20.8±0.2*	289.3±0.4*
L48QTnC ^{T53C} _{IAANS}	260±6*	0.86±0.01	7.0±0.1*	268 ±15*
M81QTnC ^{T53C} _{IAANS}	3188 ± 205*	0.72±0.03	67.7±0.8*	437±30*

Values marked with * are significantly different from their respective control values (P<0.05).

Table 2

Effects of TnC mutations on the Ca^{2+} binding properties of the reconstituted thin filaments in the absence and presence of myosin S1.

Protein	TF Ca^{2+} K _d (nM)	TF Hill coefficient	TF Ca^{2+} K _{off} (/s)	TF+S1 Ca^{2+} K _d (nM)	TF+S1 Hill coefficient	TF+S1 Ca^{2+} K _{off} (/s)
TnC ^{T53C} _{IAANS}	5027±97	1.45±0.03	102±1	1007±72	1.00±0.03	12.6±0.1
F20QTnC ^{T53C} _{IAANS}	6803±604	1.38±0.02	221±12*	8598±250*	0.93±0.01	42±1*
V44QTnC ^{T53C} _{IAANS}	841±124*	0.87±0.04*	22.2±0.3*	522±59*	0.97±0.04	6.2±0.1*
M45QTnC ^{T53C} _{IAANS}	449±33*	1.46±0.08	31.9±0.5*	814±50	1.02±0.09	2.7±0.1*
L48QTnC ^{T53C} _{IAANS}	168±7*	1.7±0.1	22.9±0.5*	241±11*	0.94±0.05	2.1±0.1*
M81QTnC ^{T53C} _{IAANS}	4468±129*	1.02±0.05*	199±7*	1403±61*	0.91±0.01*	35.7±0.6*

Values marked with * are significantly different from their respective control values ($P < 0.05$).

Table 3

Effects of TnC mutations on the actomyosin ATPase activity.

Protein	ATPase activity at pCa 9.0 (mol P _i /s)/mol S1	ATPase activity at pCa 4.0 (mol P _i /s)/mol S1	ATPase Ca ²⁺ K _d nM	ATPase Hill Coefficient
TnC ^{T53C} _{IAANS}	0.015±0.001	0.059±0.001	969±53	0.96±0.03
F20QTnC ^{T53C} _{IAANS}	0.028±0.002*	0.036±0.004*	ND	ND
V44QTnC ^{T53C} _{IAANS}	0.026±0.001*	0.056±0.001	167±6*	1.50±0.15
M45QTnC ^{T53C} _{IAANS}	0.020±0.001*	0.044±0.001*	197±16*	1.93±0.06*
L48QTnC ^{T53C} _{IAANS}	0.024±0.001*	0.052±0.003	158±11*	1.36±0.17
M81QTnC ^{T53C} _{IAANS}	0.019±0.001*	0.051±0.002*	1173±254	0.79±0.09

Values marked with * are significantly different from their respective control values (P<0.05).